

# Acute Effects of Brain Radiation in Children Evaluated by Diffusion Tensor Imaging

F. Tannazi<sup>1</sup>, T. McNutt<sup>2</sup>, S. Ardekani<sup>3</sup>, L. J. Brant<sup>4</sup>, D. Bonekamp<sup>1</sup>, O. Shokek<sup>2</sup>, K. Cohen<sup>5</sup>, M. Wharam<sup>2</sup>, S. Mori<sup>6</sup>, and A. Horska<sup>1</sup>

<sup>1</sup>The Russel H. Morgan Department of Radiology and Radiological Sciences, Johns Hopkins University School of Medicine, Baltimore, MD, United States, <sup>2</sup>Department of Radiation Oncology, Johns Hopkins University School of Medicine, Baltimore, MD, United States, <sup>3</sup>Institute of Computational Medicine, Johns Hopkins University, Baltimore, MD, United States, <sup>4</sup>NIH/NIA/GRC, Baltimore, MD, United States, <sup>5</sup>Department of Oncology, Johns Hopkins University School of Medicine, Baltimore, MD, United States, <sup>6</sup>Kennedy Krieger Institute, Johns Hopkins University School of Medicine, Baltimore, MD, United States

## Introduction:

New developments in treatment of primary brain tumors, the most common solid malignancies of childhood, have contributed to significant improvements in long term cure rate. However, with improving the survival, complications of treatments become increasingly evident. In particular, radiation therapy to the brain, even if administered at relatively low doses, has been associated with a spectrum of adverse acute, early delayed, and late effects. The dominant features of radiation injury are white matter pathologies ranging from demyelination to necrosis and vascular abnormalities. Diffusion tensor imaging (DTI) is a non-invasive method that can provide unique information on radiation-induced white matter pathology.<sup>1-3</sup> The goals of our prospective longitudinal DTI study were to evaluate white matter injury in children receiving RT for treatment of brain tumors, and to determine the relationship between changes in fractional anisotropy (FA) and radiation doses delivered to specific white matter regions.

## Methods:

We examined 9 pediatric patients (3 females, age ranges 5.5-19.3 years) who received radiation to the brain. The diagnoses included pontine glioma (n=1), medulloblastoma (posterior fossa, n=3), malignant glioma (frontal lobe, n=1), germinoma (suprasellar, n=2), pilocytic astrocytoma (hypothalamic region, n=1), and myxopapillary ependymoma (lower spine, n=1). The control group was comprised of 16 healthy children (9 females, age range 5.5-18.3 years). Control children were carefully screened for attention deficit hyperactivity disorder, learning disability and other psychopathology. All subjects were examined twice; the interval between the scans for the controls was 6 months; the patients were examined before and 6 months after the end of radiation therapy. MRI was performed using a standard birdcage head coil at 1.5 Tesla. DTI data were acquired with a single-shot spin echo planar sequence with 15 non-collinear diffusion gradient directions ( $b=1000 \text{ s/mm}^2$ ) and two  $b=0 \text{ s/mm}^2$  images. The following parameters were used: 24 axial slices, parallel to the anterior commissure - posterior commissure line,  $96 \times 96$  acquisition matrix, FOV  $240 \text{ mm}^2$ , 5 mm slice thickness, no gap. FA and color maps were calculated from raw data using the in-house developed software DTI Studio (<http://lbam.med.jhmi.edu>). Polygonal ROIs outlining each tract were drawn on the color maps two times and the measurements were averaged after overlaying the ROIs on the FA maps. Examined fiber tracts included cerebral peduncle, temporal white matter, frontal white matter, anterior and posterior limb of the internal capsule, anterior white matter, temporo-occipital white matter, superior longitudinal fasciculus, corona radiata, superior fronto-occipital fasciculus, cingulum and centrum semiovale, and genu, body, and splenium of the corpus callosum.<sup>4</sup> The majority of patients received cranio-spinal irradiation (whole brain and spine). Some patients also underwent a boost treatment to the posterior fossa and some patients received radiation only to a targeted region of the brain. Therefore, a wide range of doses was delivered to the specific regions identified on the FA maps across the study patients. In order to assess the dose delivered to the various regions, the FA maps were imported into the Pinnacle Treatment Planning System (Philips Medical Systems, Madison WI) and registered with the treatment plan using the CT simulation scan. The FA regions were contoured and the dose distribution in each region was evaluated. The relative change in FA between the two scans was calculated according to  $\Delta FA = (FA_{\text{First}} - FA_{\text{Second}}) / FA_{\text{First}}$ . Linear mixed effects (LME) analyses were used to identify factors related to changes in FA in the 15 examined brain regions. The following factors (and their interactions) were considered: group, time (initial and follow-up scan), hemisphere, region, and radiation dose.

## Results:

The LME analyses revealed highly significant differences in FA between the patients and controls, between the two examinations, and among the brain regions

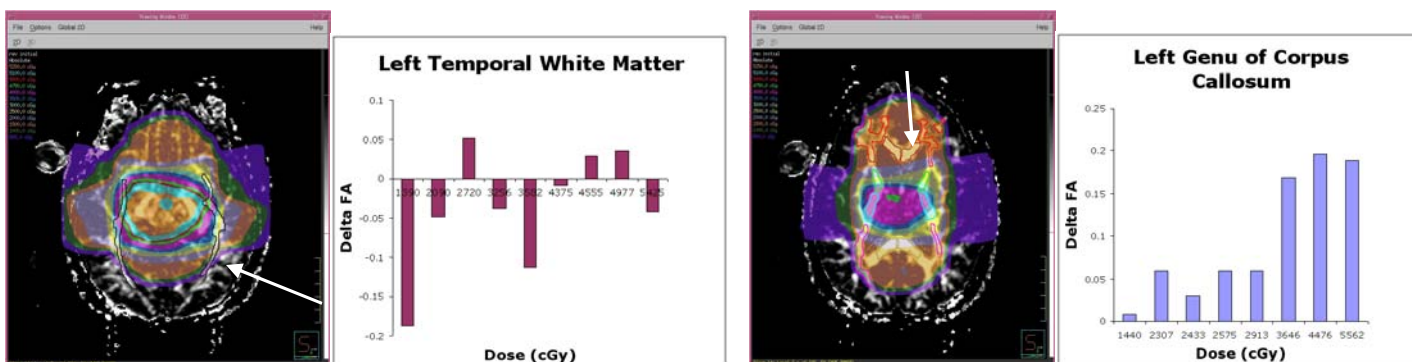


Fig. 1. Left: Map of radiation dose overlaid on FA map at the level of temporal white matter. Right: Bar graph representing distribution of  $\Delta FA$  versus radiation dose for the temporal white matter in the left hemisphere.

Fig 2. Left: Radiation dose map overlaid on FA map at the level of the corpus callosum. Right: Bar graph representing distribution of  $\Delta FA$  versus radiation dose for the genu of the corpus callosum in the left hemisphere.

(interaction terms group x time,  $p < 0.001$ ; group x region,  $p < 0.001$ ; time x region,  $p = 0.004$ ). In healthy children, the detected FA changes (on average  $9.2 \pm 3.5\%$ ) were comparable to or slightly higher than FA variability determined previously for our protocol (coefficient of variation  $\sim 5\%$ )<sup>4</sup>. In contrast, FA changes in patients were higher (up to 30%) but a large variability in  $\Delta FA$  was observed, both among regions and between hemispheres. In regions proximal to the center of the radiation field (posterior fossa, posterior temporal and occipital regions),  $\Delta FA$  was both positive and negative and independent on radiation dose (Fig. 1). However, in several regions distant from the center of the radiation field (and tumor site)  $\Delta FA$  was positive (indicating decrease in FA after RT, Fig 2) and increased with radiation dose (left genu of the corpus callosum,  $p < 0.0009$ ; left anterior white matter,  $p = 0.01$ ).

## Discussion:

We hypothesized that radiation injury will result in FA decrease and that higher radiation doses will lead to larger changes in regional FA values. However, our initial results indicate that in the acute phase of radiation injury, FA changes may not only be associated with radiation doses but may largely vary among brain regions (and patients). Increase in FA appears to be an unexpected finding; however, our results are in agreement with data reported recently in a follow-up DTI study in two patients treated with radiation.<sup>5</sup> The previous study<sup>5</sup> also reported variations in regional white matter susceptibility to RT. We believe that the high variability in FA for the ROIs near the center of the radiation field early post-radiation is a result of tissue injury, and, in many cases, due to surgery. In contrast, the regions distant from the center of the radiation field (in particular in regions with densely packed fibers), FA decreased, as hypothesized.

The initial data from our study indicate that DTI can be used to monitor changes in white matter structure after brain radiation in children and may, in the future, provide vital information on regional tissue susceptibility and dose threshold, important for radiotherapy planning.

## References:

1. Khong P.L., et al. AJNR Am. J. Neuroradiol. 24: 734-740 (2003).
2. Khong P.L., et al. Radiology 236: 647-652 (2005)
3. Leung L.H., et al. NeuroImage 21: 261-268 (2004)
4. Bonekamp D, et al. NeuroImage (2006); in press.
5. Qiu D, et al. NeuroImage 31:109 (2006)

Supported by NIH Grant R01 NS042851 and RR 00052.